Downloaded from gsabulletin.gsapubs.org on 30 January 2009

Geological Society of America Bulletin

Carbonate accretionary lapilli in distal deposits of the Chicxulub impact event

Thomas E. Yancey and Renald N. Guillemette

Geological Society of America Bulletin 2008;120;1105-1118
doi:10.1130/B26146.1

Email alerting services click www.gsapubs.org/cgi/alerts to receive free email alerts when new articles cite this article

Subscribe click www.gsapubs.org/subscriptions/index.ac.dtl to subscribe to Geological Society of America Bulletin

Permission request click http://www.geosociety.org/pubs/copyrt.htm#gsa to contact GSA

Copyright not claimed on content prepared wholly by U.S. government employees within scope of their employment. Individual scientists are hereby granted permission, without fees or further requests to GSA, to use a single figure, a single table, and/or a brief paragraph of text in subsequent works and to make unlimited copies of items in GSA's journals for noncommercial use in classrooms to further education and science. This file may not be posted to any Web site, but authors may post the abstracts only of their articles on their own or their organization's Web site providing the posting includes a reference to the article's full citation. GSA provides this and other forums for the presentation of diverse opinions and positions by scientists worldwide, regardless of their race, citizenship, gender, religion, or political viewpoint. Opinions presented in this publication do not reflect official positions of the Society.

Notes

© 2008 Geological Society of America

THE GEOLOGICAL SOCIETY OF AMERICA

Carbonate accretionary lapilli in distal deposits of the Chicxulub impact event

Thomas E. Yancey†
Renald N. Guillemette*
Department of Geology and Geophysics, Texas A&M University, College Station, Texas 77843-3115, USA

ABSTRACT

The petrography and chemical composition of carbonate accretionary particles of Chicxulub impact origin are described from Cretaceous-Paleogene boundary deposits at Brazos River, Texas, and Bass River borehole, New Jersey. The particles consist of lapilli and lapilli fragments ranging in size from 0.05 to 0.3 cm; they are white in color, have an accretionary fabric at several scales, and are composed of micrometer-sized microspar of low-Mg calcite with an elevated sulfur content. The internal aggregate microfabric indicates that they formed by accretion of small solid particles, suggesting an origin from carbonate crystals generated within the vapor plume of the Chicxulub impact. Carbonate accretionary lapilli occur with altered glass spherules in Cretaceous-Paleogene boundary deposits at sites in Texas and northern Mexico and in the spherule layer in New Jersey, indicating that a large amount of particulate carbonate was present within the impact plume.

Keywords: accretionary lapilli, impact spherules, Chicxulub, Cretaceous-Paleogene boundary.

INTRODUCTION

Ejecta materials produced by the Chicxulub impact event include many types and sizes of particles, ranging from large blocks of bedrock within or near the crater (Alvarez et al., 1995; Ocampo et al., 1996; Claeys et al., 2002) to tiny spinel-bearing microkrystite spherules and shocked quartz grains found far from the impact site (Kyte et al., 1996; Rocchia et al., 1996). Apart from shocked quartz, the most recognized ejecta particles are small (0.1–0.3 cm) altered glass spherules formed from silicate melt (Kyte et al., 1996; Smit et al., 1996), most of which have now been replaced by clay, calcite, and/or pyrite, and only a few of which contain remnants of unaltered glass (Koeberl, 1993). Altered glass spherules occur in the Cretaceous-Paleogene boundary deposits at Brazos River, Texas, but examination of the deposits shows that rounded particles of carbonate composition (Fig. 1A) with a similar size range are also common in the ejecta-rich beds and resedimented sandstone beds (Yancey, 2002; Guillemette and Yancey, 2006). Although this co-occurrence suggested an ejecta origin for these carbonate particles, they had few obvious features to indicate their origin until they were examined with high-magnification electron imaging. The ejecta origin is established by examination of the interiors of the particles, which reveal a microgranular accretionary fabric comparable to the fabric of large carbonate accretionary lapilli reported from deposits near the Chicxulub impact site (Ocampo et al., 1996; Fouke et al., 2002; Pope et al., 2005; Salge, 2007a, 2007b) and from deposits of the Late Devonian Alamo impact (Warme and Kuehner, 1998; Warme et al., 2002; Morrow et al., 2005). Another indication of their ejecta origin is the observation that they occur only in sediments of the Cretaceous-Paleogene boundary deposits and are not found in sands or coarse-grained sediments above or below the boundary deposits. Carbonate accretionary lapilli are recognized in section by their accretionary fabric and in unweathered hand samples by their uniform white appearance. The presence of carbonate accretionary lapilli in ejecta deposits located ~1000 km from the impact crater (Fig. 2) is unexpected, but further investigation reveals they are also present in a much more distant site at Bass River borehole, New Jersey (see Olsson et al., 1997, 2002, for site description), as well as at nearby sites in northern Mexico (Guillemette and Yancey, 2007).

These occurrences indicate that carbonate accretionary particles of small size (0.05–0.3 cm) are a common component of Chicxulub impact ejecta in locations distant from the impact crater. In basal ejecta-rich beds of the Brazos River section (Figs. 1C and 1D), carbonate accretionary lapilli compose ~25% of the coarse ejecta fraction (altered glass spherules plus carbonate accretionary lapilli). In resedimented coarse sands (Figs. 1E and 1F), carbonate accretionary particles (lapilli and sublapilli) make up ~50% of the total ejecta fraction, and in fine-grained hummocky cross-bedded sands (Fig. 3), sublapilli particles are common and total 100% of the ejecta fraction.

Small carbonate ejecta particles in Cretaceous-Paleogene boundary deposits along the north and west margins of the Gulf of Mexico have been reported by Smit et al. (1996) and Schulte et al. (2006) as examples of bedrock clasts or possibly accretionary lapilli (Schulte et al., 2006). However, examination of the Brazos River deposits reveals that most have an accretionary fabric that is atypical of sedimentary carbonate. They have an unusual white granular appearance in reflected light (Fig. 1A) and an internal aggregate-like accretionary fabric in thin section (Fig. 3) that is similar to the fabric present in larger impact-generated accretionary lapilli (Pope et al., 1999, 2005; Warme and Kuehner, 1998; Warme et al., 2002). Carbonate accretionary particles in the Brazos River deposits range in size from 0.05 to 0.3 cm diameter, and most have a diameter of 0.1–0.2 cm. Although this is mostly below the 0.2 cm lower size limit of tephra lapilli particles, the term accretionary lapilli is applied as a group term for impact-generated accretionary particles of a large size range, including sizes above and below the tephra lapilli size limits (Pope et al., 1999, 2005; Warme and Kuehner, 1998; Warme et al., 2002). Small to very small accretionary particles of Chicxulub impact origin are common in the Albion Island Formation spheroid and diamictite beds exposed along the Mexico-Belize border, and these are identified as accretionary lapilli (Pope et al., 2005). This is a reasonable application of the term, despite the size

†E-mail: yancey@geo.tamu.edu.
*E-mail: guillemette@geo.tamu.edu.

GSA Bulletin; September/October 2008; v. 120; no. 9/10; p. 1105–1118; doi: 10.1130/B26146.1; 10 figures; 2 tables.

For permission to copy, contact editing@geosociety.org
© 2008 Geological Society of America

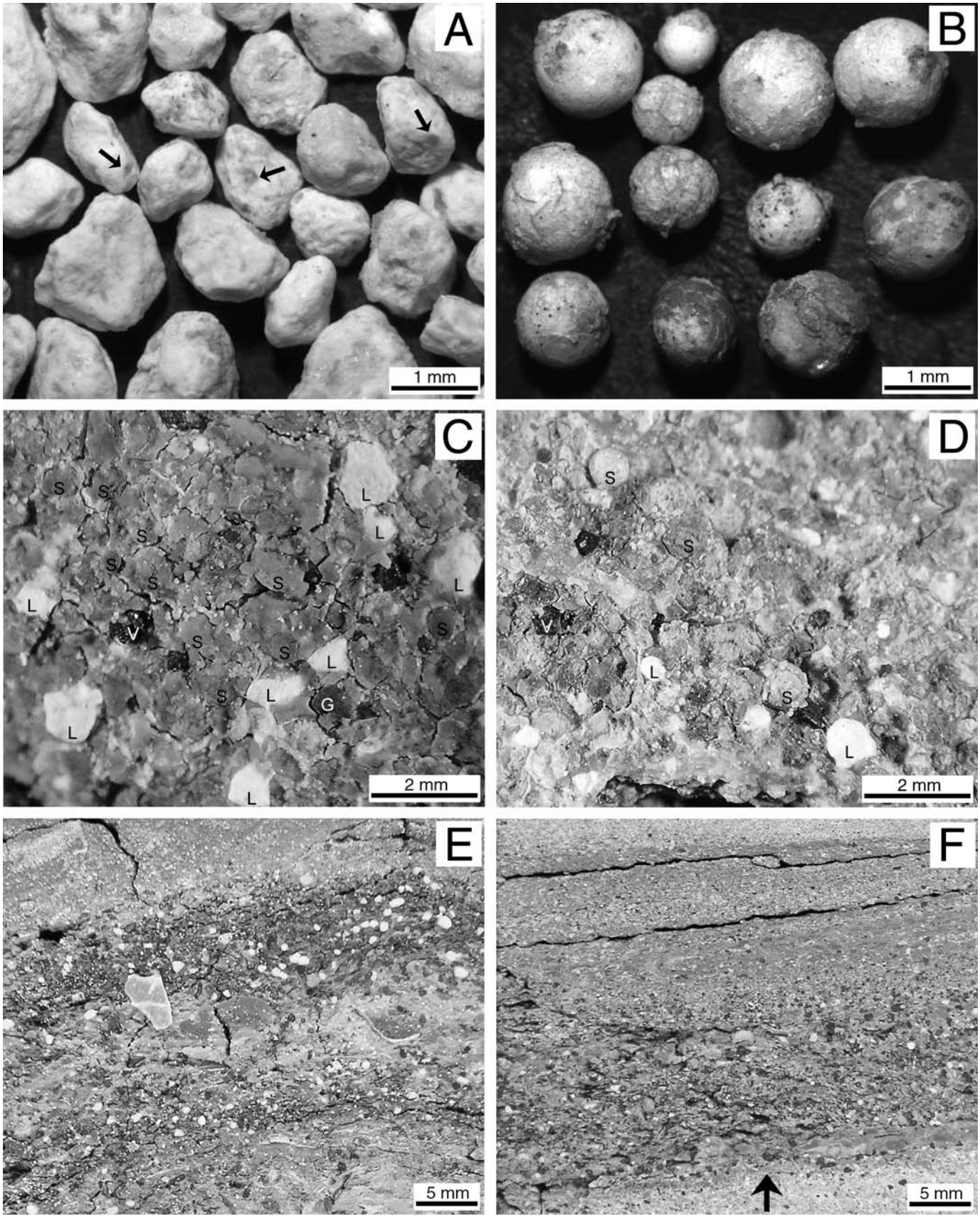
A
1 mm
B
1 mm
C
S
L
V
G
2 mm
D
S
L
V
2 mm
E
5 mm
F
5 mm

Figure 1. Reflected-light views of ejecta and ejecta-bearing sediment layers of Cretaceous-Paleogene boundary deposits, Brazos River, Texas. (A) Carbonate accretionary sublapilli and lapilli fragments, showing microgranular texture, dark patches with smectite concentration (arrows), and angular broken surfaces present on most particles. Spherule-rich layer in Brazos River section RB4B, Brazos River. (B) Calcite-replaced bubble-bearing glass spherules. Spherule-rich layer in Brazos River section RB4B, Brazos River. (C) Eroded surface of spherule-rich layer; plain white irregular sediment grains are carbonate accretionary sublapilli and lapilli fragments (L), dark black irregular sediment grains are pieces of fish bone (V) or glauconite pellets (G), and grayish rounded sediment grains are smectite-replaced bubble-bearing glass spherules (S); other sediment grains are indistinct. Darting Minnow section, 50 cm level, Darting Minnow Creek, Brazos River. (D) Eroded surface of spherule-rich layer; dull white spherule in upper left is a carbonate-replaced glass spherule (S); plain white sediment grain in lower right is a carbonate accretionary sublapillus (L); most of the grayish rounded sediment grains exposed on surface are cross sections of smectite-replaced or calcite-replaced bubble-bearing glass spherules (S); and black irregular sediment grains are pieces of fish bone (V). Darting Minnow section, 50 cm level, Darting Minnow Creek, Brazos River. (E) Cut surface of core showing concentration of white carbonate accretionary lapilli, sublapilli, and lapilli fragments in spherule-bearing sand layer of Cretaceous-Paleogene boundary deposits. Sand layers contain carbonate accretionary lapilli and lapilli fragments, altered bubble-bearing glass spherules, fossil fragments, glauconite pellets, and lithoclasts in smectite matrix. Flat angular object on surface is a flake of calcitic oyster shell. Mullinax #1 core, Brazos River. (F) Cut surface of core showing concentration of white carbonate accretionary sublapilli and lapilli fragments in spherule-bearing fining-upward sand layers with sharp basal contact (arrow) in Cretaceous-Paleogene boundary deposits; cross-bedding in upper part of photo is part of a hummocky cross-bedded layer in fining-upward unit; sand layers contain carbonate accretionary sublapilli and lapilli fragments, altered bubble-bearing glass spherules, fossil fragments, glauconite pellets, and lithoclasts in smectite matrix. Mullinax #1 core, Brazos River.

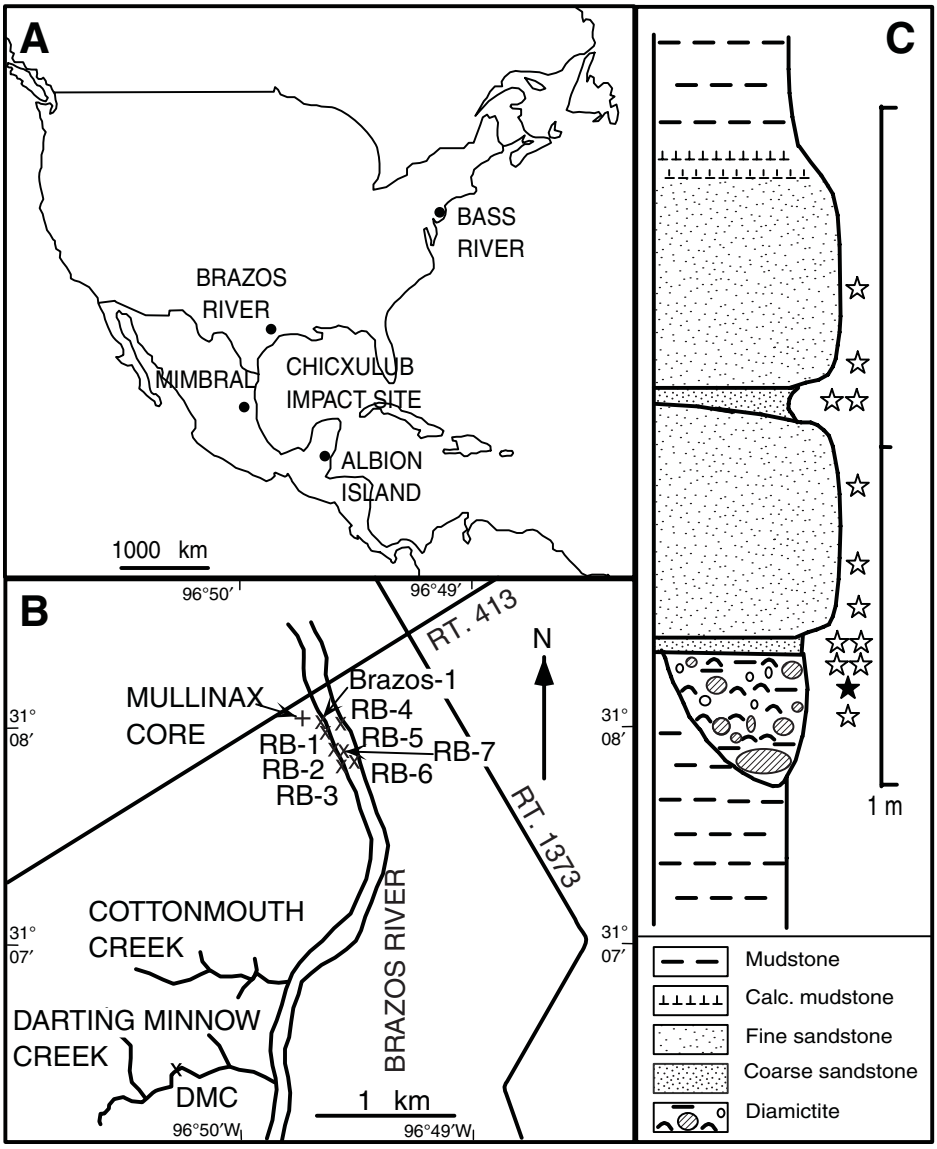

Figure 2. (A) Location map of sites with carbonate accretionary lapilli and sublapilli grains studied here, shown in relation to the Chicxulub impact site and Albion Island Formation exposures. (B) Sampling sites at Brazos River, Texas. (C) Stratigraphy of the Cretaceous-Paleogene boundary deposits, Brazos River, Texas. Stars indicate levels with carbonate accretionary lapilli and sublapilli; double stars indicate greater abundance. Figure was modified from Yancey (1996).

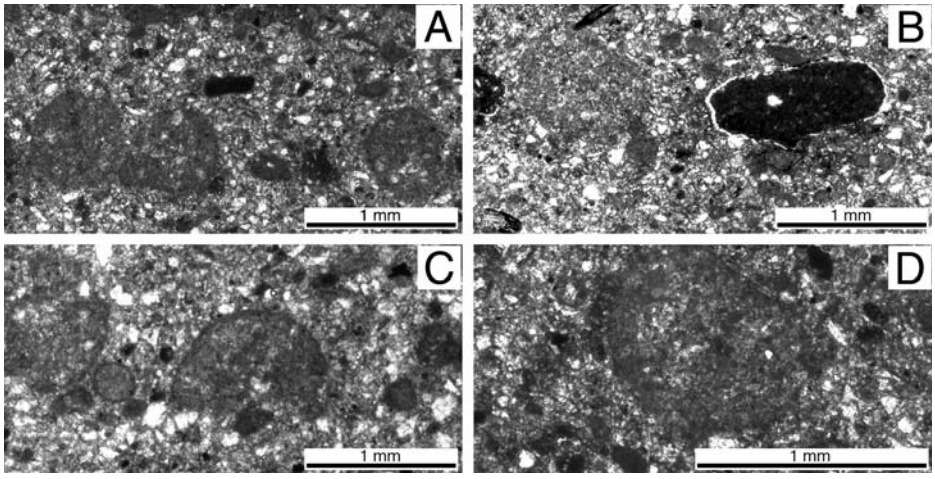

Figure 3. Plane-polarized light microphotographs of an ejecta-rich fine sand layer, Darting Minnow section, 100 cm level, Darting Minnow Creek, Brazos River, Texas. (A) Three rounded carbonate accretionary sublapilli and fragments in quartzose sand containing grains of varied composition, including small mudstone clasts, fossil fragments, and glauconite pellets; small clear grains in matrix are detrital quartz. (B) Contrasting appearance of a rounded carbonate accretionary sublapillus (left side of photo) and a mudstone clast (right side); clear white spot in mudstone clast is carbonate-filled chamber of microfossil; sediment composition as above. (C) Three carbonate accretionary sublapilli and fragments (center sublapillus is very small) in quartzose sand; sublapillus in center of photo has broken surface aligned parallel to bedding; note the dark appearance of rims when viewed in transmitted light; sediment composition as above. (D) Carbonate accretionary lapillus showing accretionary fabric and dark rim; compare fabric with backscattered electron images of lapilli in Figures 4 and 5; sediment composition as above.

implications of the word lapilli, because accretionary lapilli are formed by a growth process that aggregates small and very small particles contained in a particle-laden suspension. The growth process is not inherently size limiting and growth can continue or stop at any time. The smaller particles (sublapilli) examined either did not grow to lapilli size or are fragments of lapilli, broken during transport.

DESCRIPTION AND ANALYSIS OF CARBONATE ACCRETIONARY LAPILLI

Carbonate accretionary lapilli and sublapilli at the Brazos River and Bass River borehole sites are composed mostly of minute crystals of low-Mg calcite, and they have an accretionary, aggregate fabric at both the micro- and mesoscopic scales. The aggregate texture characteristic of these particles can be recognized in thin sections (Fig. 3) and is well displayed in backscattered electron (BSE) images (Figs. 4 and 5). The smallest components are 1–4-μm-size crystals of low-Mg calcite (Figs. 5F and 5G) that form the bulk of the accretionary particles, accompanied by 5–10 μm calcite crystals in some of the lapilli (Figs. 5C and 5F). Carbonate accretionary lapilli and sublapilli contain smaller aggregates of many sizes, ranging from 10 to 20 μm rounded clusters (Figs. 4F and 5E) composed of micrometer-sized calcite crystals to large, 500 μm, heterogeneous aggregates (Figs. 4B and 4C). The larger aggregates are composed of variable proportions of low-Mg calcite crystals, smectite masses, and smaller aggregates of calcite crystals. Some of the midsized aggregates are composed dominantly of smectites and are interpreted as altered silicic glass (Fig. 5C and 5E). Fabric showing multiple episodes of aggregation is shown in Figures 5A, 5B, and 5D. The lapilli show little zoning or banding apart from an outer rim, which is seen as darker zones in thin-section photographs (Figs. 3C and 3D) and as whiter rims in BSE images (Figs. 4F and 5E). This outer rim is not noticeable in reflected light, except as a smoother surface on nonabraded grains. The absence of concentric banding in the interiors of these small particles is consistent with their small size and the fact that small components are blocky or rounded in shape (Figs. 4A, 4C, 4D, 5A, 5B, 5D, and 5E). Multiple images of Brazos River and Bass River carbonate accretionary lapilli are presented in Figures 4 and 5 to illustrate the characteristic range of microfabric of these particles.

Chemical analyses were carried out on a Cameca SX50 electron microprobe equipped with four wavelength-dispersive spectrometers (WDS) and a Princeton Gamma-Tech energy-dispersive spectroscopy (EDS). WDS quantitative analyses on carbonates were performed with a 15 kV, 10 nA, 10 μm beam using well-characterized microprobe standards obtained from the Smithsonian Institution, Washington, D.C. (Jarosewich, 2002). X-ray elemental distribution maps were obtained using WDS spectrometers with a 15 kV, 10 nA beam focused to the smallest possible size (<1 μm). The stage was rastered in a 512 × 512 grid beneath a fixed beam to acquire 0.1 cm X-ray maps, while the beam was deflected over a fixed stage to acquire the <100 μm maps; dwell time on each pixel was 15 ms.

Chemical analyses of carbonate accretionary lapilli and sublapilli from Brazos River and Bass River, along with comparative analyses of diagenetic and pedogenic materials, are presented in Table 1. These analyses reveal that accretionary lapilli carbonate can be distinguished from other carbonate by an elevated sulfur content, ranging from 0.3 to 0.8 wt% SO_3, compared with secondary diagenetic calcite, containing 0.03 wt% SO_3 or less. Even the 0.03 wt% SO_3 content in one of our analyses is suspected to be anomalously high because it was derived from a pedogenic soil nodule containing some pedogenic gypsum crystals. Of the 25 analytical points on this soil nodule, two points were removed from the set because of greatly elevated sulfur content, contrasting with low sulfur content of other points, indicating in-mixing of gypsum in the nodule. Within accretionary lapilli carbonate, elevated sulfur content is more dispersed and consistent with the interpretation that sulfate evaporites at the impact site contributed to the vapor cloud in which the accretionary particles formed.

Two other compositional features of the accretionary lapilli deserve mention. Elemental mapping shows that some of them have areas with elevated Mg content (Figs. 6A, 6B, and 6C); 10-μm-diameter WDS quantitative analyses within these areas of high-Mg content have elemental totals that are abnormally high, well in excess of 100 wt% when calculated as carbonate. Energy-dispersive X-ray (EDS) spectra of the most Mg-rich 1-μm-sized spots show that the Mg/Ca ratio is too high for these areas to be dolomite (Figs. 6 and 7). The presence of $MgCO_3$ is possible but unlikely, because when the Mg content of these points is recalculated as MgO instead of $MgCO_3$ (Table 2), analytical totals are very close to 100 wt%, indicating that the Mg may be present in the form of minute crystals of MgO. If present, the MgO occurs as crystals <1 μm in diameter. The formation of residual oxide MgO has been predicted to

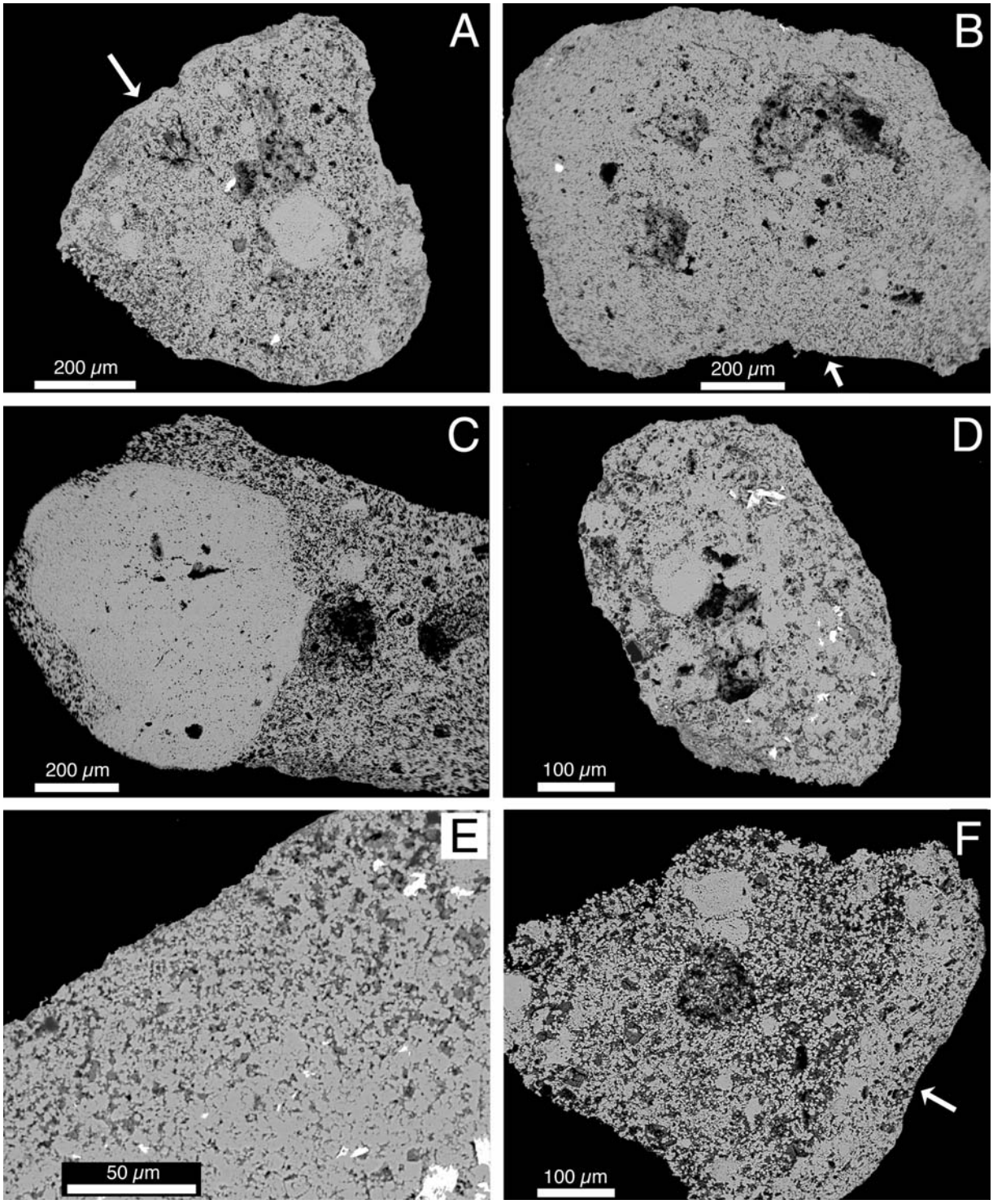

Figure 4. Backscattered electron (BSE) images of carbonate accretionary sublapilli, spherule-rich layer in Brazos River sections RB2 (A–E) and RB4B (F), Brazos River, Texas. (A) Carbonate accretionary sublapillus fragment composed of 20–150 μm calcite aggregates; part of original rim zone on upper left side (arrow) has been retained. (B) Carbonate accretionary lapillus fragment retaining original rim zone except on broken lower margin (arrow), composed of small calcite aggregates and smectite masses of replaced silicic glassy particles (dark areas); large aggregate in right area has heterogeneous composition. (C) Fragment of carbonate accretionary lapillus fragment containing a smaller carbonate accretionary mass with accretionary fabric. (D) Small carbonate accretionary sublapillus composed of a heterogeneous group of calcite aggregates and smectite-replaced silicic glass; note small crystal laths of diagenetic barite (bright white tabular crystals). (E) Detail of marginal rim zone of a carbonate accretionary lapillus fragment showing smaller size (1–4 μm) of calcite crystals in rim zone contrasting with 5–10 μm crystals in inner zone; small well-defined crystal laths of diagenetic barite are present (bright white). (F) Fragment of carbonate accretionary sublapillus showing accretionary fabric and rim zone (arrow) with denser concentration of small calcite crystals; rim zone appears whiter due to concentration of calcite.

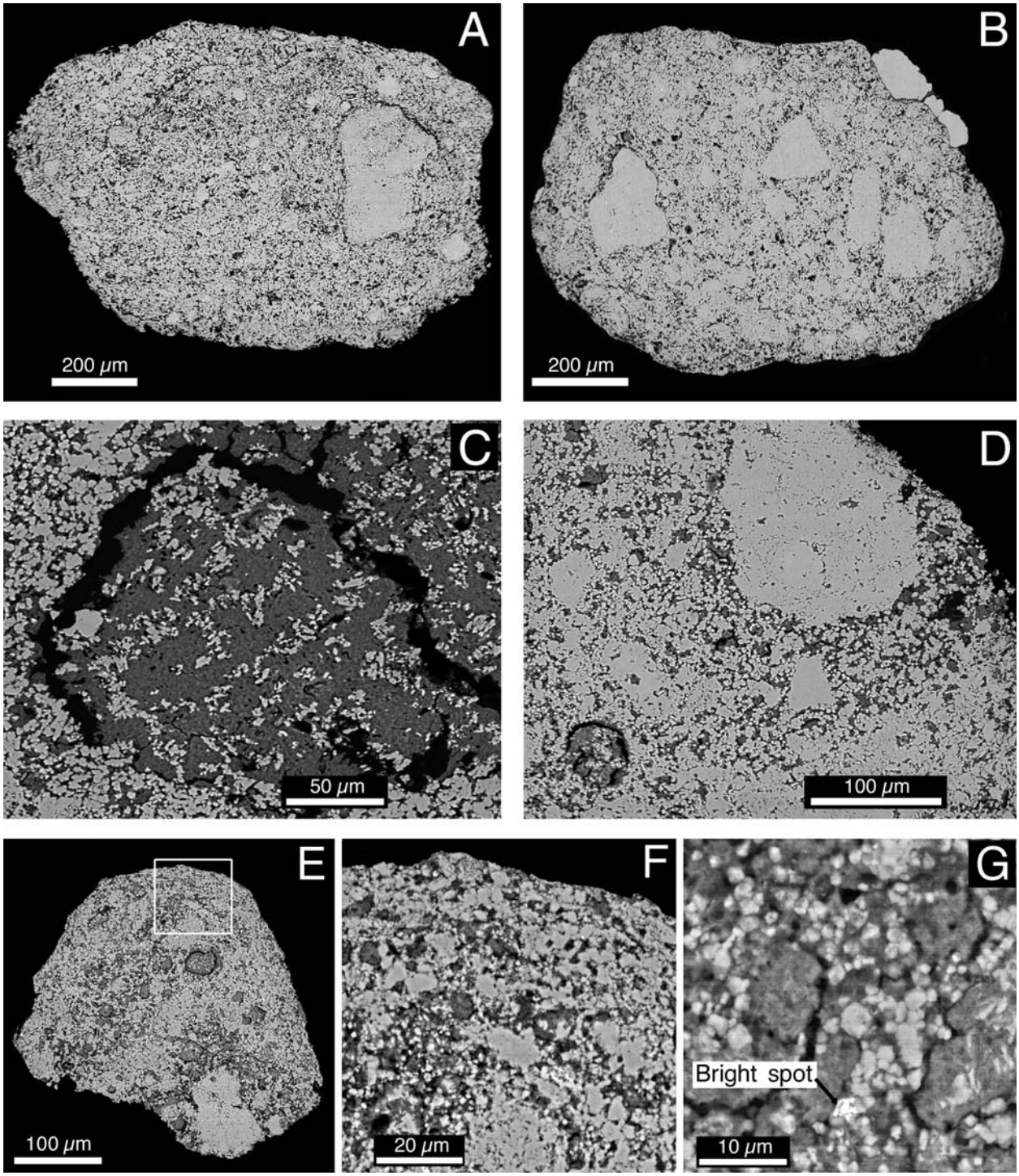

Figure 5. Backscattered electron (BSE) images of carbonate accretionary sublapilli, spherule-rich layer in Brazos River section RB4B, Brazos River, Texas (A, B), in Mullinax #1 core, Brazos River, Texas (C, D), and spherule-rich layer in Bass River borehole, New Jersey (E–G). (A) Carbonate accretionary sublapillus fragment composed of small and large calcite aggregates; largest aggregate (right side) has an accretionary fabric of variably sized smaller aggregates. (B) Carbonate accretionary sublapillus fragment composed of small and large calcite aggregates. (C) Smectite mass with aggregate fabric outlined by bands of minute calcite crystals; this sample is part of a large carbonate accretionary lapillus. (D) Portion of carbonate accretionary lapillus containing smaller calcite aggregates; aggregate in upper right shows well-developed accretionary fabric. (E) Carbonate accretionary sublapillus fragment composed of small calcite aggregates and smectite masses; original rim zone is preserved on upper margin. (F) Enlargement of rim zone of the carbonate accretionary sublapillus illustrated in E, showing smallest (few μm) calcite crystals and small (10–20 μm) calcite aggregates mixed with equally small masses of smectite-replaced silicic glass. (G) Enlargement of a carbonate accretionary sublapillus, showing low-Mg calcite crystals and smectite-replaced silicic glass masses and one bright spot. Bright spot is calcite with higher S, Mg, and Si concentration.

TABLE 1. CHEMICAL COMPOSITION* OF CARBONATE ACCRETIONARY LAPILLI AND SUBLAPILLI FROM BRAZOS RIVER, TEXAS,† AND BASS RIVER BOREHOLE, NEW JERSEY, COMPARED WITH SECONDARY CALCITE OF DIAGENETIC ORIGIN (SECTIONS RB4B, DMC 50) AND OF PEDOGENIC ORIGIN FROM BROWNWOOD, TEXAS

Analysis	$CaCO_3$ (wt%)	MgO (wt%)	$FeCO_3$ (wt%)	$MnCO_3$ (wt%)	$SrCO_3$ (wt%)	SO_3 (wt%)	Na_2O (wt%)	Al_2O_3 (wt%)	SiO_2 (wt%)	Total (wt%)
Accretionary Lapilli										
RB2 Accretionary										
Mean	94.0	2.86	0.13	0.04	0.09	0.80	0.06	0.20	0.64	98.8
Std dev (99 pts, 9 grains)	2.8	1.86	0.09	0.03	0.04	0.34	0.02	0.22	0.54	0.9
RB4B Accretionary										
Mean	96.5	0.71	0.81	0.27	0.12	0.40	0.04	0.16	0.34	99.4
Std dev (34 pts, 6 grains)	1.8	0.69	0.93	0.30	0.04	0.25	0.02	0.14	0.33	0.7
RB6 Accretionary										
Mean	95.4	0.65	1.30	0.39	0.17	0.30	0.02	0.10	0.24	98.6
Std dev (48 pts, 3 grains)	2.4	0.64	1.11	0.30	0.07	0.28	0.01	0.11	0.29	1.5
Mull 14-16 Accretionary										
Mean	96.0	0.94	0.60	0.22	0.15	0.67	0.05	0.18	0.38	99.2
Std dev (51 pts, 11 grains)	2.4	1.15	0.91	0.25	0.07	0.39	0.03	0.27	0.56	1.3
Bass River Accretionary										
Mean	97.2	0.37	0.09	0.01	0.31	0.62	0.03	0.12	0.34	99.1
Std dev (6 pts)	1.7	0.06	0.06	0.02	0.14	0.31	0.02	0.11	0.36	1.5
Bass River BSE bright§										
Mean	88.4	1.54	0.25	0.09	0.29	1.13	0.06	0.92	2.43	95.1
Std dev (7 pts)	4.9	0.77	0.14	0.08	0.18	0.47	0.03	0.45	1.46	2.8
Secondary Calcite										
RB4B Void fill										
Mean	96.4	0.48	1.51	0.42	0.12	0.04	0.01	0.03	0.05	99.1
Std dev (7 pts, 3 grains)	2.2	0.12	1.28	0.29	0.09	0.05	0.01	0.02	0.04	1.1
RB4B Secondary crust										
Mean	96.0	0.23	1.87	0.67	0.05	0.00	0.01	0.01	0.02	98.8
Std dev (5 pts, 2 grains)	1.0	0.05	0.62	0.06	0.02	0.00	0.00	0.01	0.01	0.4
RB6 Secondary crust										
Mean	96.6	0.19	1.60	0.62	0.06	0.02	0.01	0.04	0.13	99.2
Std dev (2 pts, 1 grains)	0.7	0.06	0.27	0.03	0.01	0.00	0.01	0.04	0.09	0.9
Replaced Glass Spherules										
RB4B										
Mean	94.4	1.38	2.13	0.87	0.07	0.02	0.01	0.04	0.09	99.0
Std dev (35 pts, 5 grains)	1.1	1.05	0.69	0.54	0.03	0.03	0.01	0.06	0.12	0.6
DMC50										
Mean	95.0	0.91	2.55	0.69	0.12	0.02	0.01	0.05	0.10	99.4
Std dev (25 pts, 7 grains)	1.1	0.66	0.71	0.27	0.06	0.03	0.01	0.07	0.18	0.6
Pedogenic Nodule										
Brownwood										
Mean#	96.9	0.40	0.43	0.03	0.03	0.09	0.03	0.84	1.98	100.7
Std dev (23 pts, 1 grain)	2.1	0.18	0.20	0.04	0.04	0.06	0.03	0.50	1.37	0.7

Note: Underlined numbers are below the detection limit. Note higher concentration of sulfur in accretionary lapilli and low concentration of Mg in all samples. Analyses were carried out on a Cameca SX50 electron microprobe equipped with four wavelength-dispersive X-ray (WDS) spectrometers and a Princeton Gamma-Tech energy dispersive spectroscopy. WDS analyses on carbonates were performed with a 15 kV, 10 nA, 10-µm-diameter beam using well-characterized reference standards.

*Determined by WDS electron-microprobe analysis.

†Sections RB2, RB4B, RB6, and Mullinax #1 core.

§Smaller, backscattered electron (BSE) brighter accretionary particles.

#2 pts removed because of presence of gypsum.

TABLE 2. CHEMICAL COMPOSITION OF SEVEN DIFFERENT AREAS OF THE SAME Mg-RICH SUBLAPILLUS FROM BRAZOS RIVER SECTION RB2, BRAZOS RIVER, TEXAS*

RB2 Spherule 1	$CaCO_3$	$MgCO_3$	$FeCO_3$	$MnCO_3$	$SrCO_3$	SO_3	Na_2O	Al_2O_3	SiO_2	Total (wt%)	MgO	Total (wt%)
Area 1	92.8	10.2	0.09	0.03	0.10	0.81	0.06	0.10	0.45	104.7	4.88	99.3
Area 2	94.6	7.5	0.12	0.03	0.12	0.87	0.05	0.22	0.77	104.2	3.55	100.3
Area 3	95.0	7.7	0.10	0.02	0.11	0.85	0.05	0.09	0.35	104.2	3.65	100.2
Area 4	91.2	12.8	0.08	0.03	0.09	1.04	0.06	0.08	0.40	105.8	6.11	99.1
Area 5	92.6	9.1	0.16	0.02	0.08	0.97	0.04	0.13	0.41	103.5	4.33	98.7
Area 6	97.2	1.8	0.03	0.05	0.12	1.16	0.13	0.01	0.09	100.7	0.88	99.7
Area 7	88.2	16.0	0.18	0.07	0.12	1.02	0.07	0.28	0.85	106.7	7.62	98.4
Mean	93.1	9.3	0.11	0.04	0.11	0.96	0.07	0.13	0.48	104.3	4.43	99.4
Std dev	2.9	4.5	0.05	0.02	0.02	0.13	0.03	0.09	0.26	1.9	2.13	0.7

Note: Underlined numbers are below the detection limit.

*Mg content calculated both as a carbonate phase and as an oxide phase, showing that Mg may occur as an oxide phase in the sample. With Mg calculated as a carbonate, the analytical totals are excessive, but calculated as an oxide, the analytical totals are within range of other analyses done on spherules and standards and close to 100 wt%.

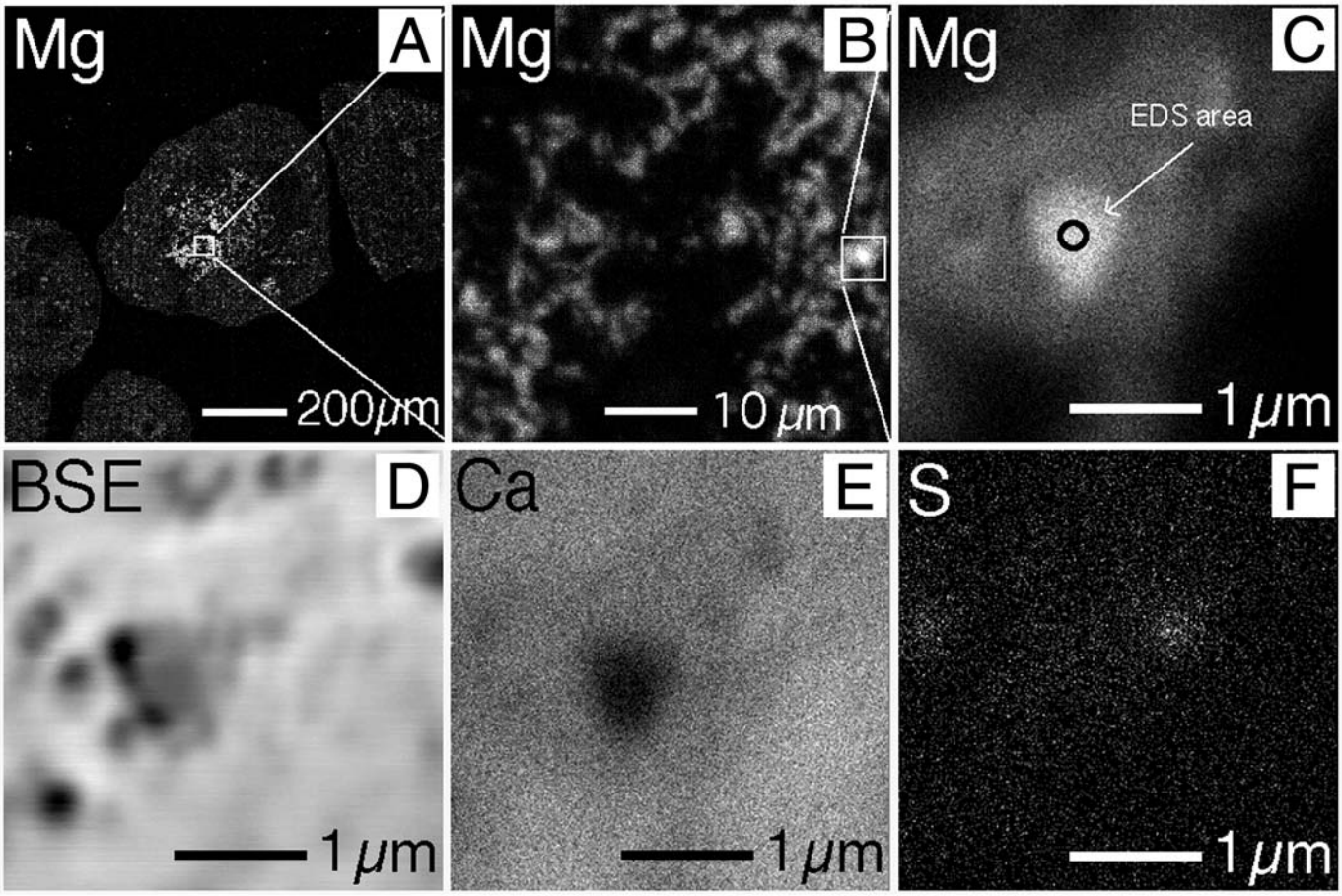

Figure 6. Wavelength-dispersive spectroscopy (WDS) X-ray and backscattered electron (BSE) images of carbonate accretionary sublapillus from Brazos River section RB2, Brazos River, Texas, showing element distribution in area of high-Mg content. (A) Mg distribution in sublapillus with area of high-Mg content (shown in box). (B) Enlargement of area with high-Mg content. (C) Enlargement of B, with outline of point of energy-dispersive spectroscopy (EDS) spectrum (shown in Fig. 7) on area of high-Mg content. (D) BSE image of same area as C. (E) Ca distribution in area of high-Mg content within sublapillus; same area as C. (F) S distribution in area of high-Mg content within sublapillus; same area as C. Image A was obtained by 2 μm step 512 × 512 stage rastering, while images B–F were acquired by <1 μm step 512 × 512 beam rastering.

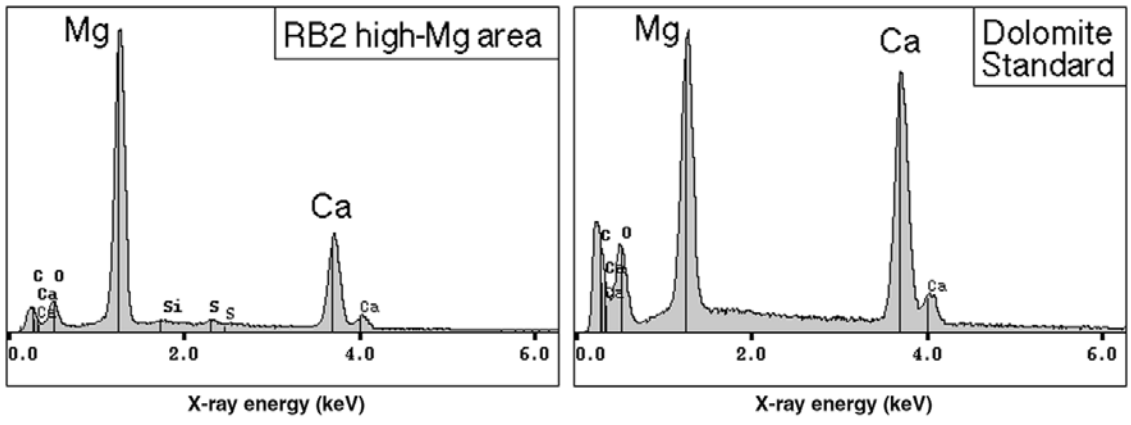

Figure 7. Energy-dispersive spectroscopy (EDS) spectrum of high-Mg area in carbonate accretionary sublapillus from Brazos River section RB2, Brazos River, Texas, compared to spectrum of stoichiometric dolomite standard USNM 10057 (Jarosewich, 2002). The minor signal of Ca in the high-Mg area spectrum results from excitation of some of the surrounding calcite because the area of high-Mg content is too small to provide a signal limited entirely to the target grain, despite focusing the beam to <1 μm.

occur during high-energy impact (Agrinier et al., 2001), and Warme et al. (2002) considered the possibility of MgO formation during the Alamo impact event, but the presence of impact-generated MgO has not been definitively demonstrated. The analyses presented here suggest the presence of MgO as submicrometer particles in Brazos River lapilli and sublapilli, but they do not provide definitive proof confirming the presence of MgO particles.

Another feature observed in Bass River lapilli fragments is the occurrence of crystals with brighter BSE reflection than most calcite (Fig. 5G). These bright spots appear to be calcite in composition but contain higher S, Mg, and Si concentrations than typical lapilli calcite. The analysis of these spots is limited by the fact that the bright spots are 1 μm or less in diameter, and they are therefore too small to be reliably analyzed by electron beam X-ray microanalysis. The elemental composition of these spots deserves further study.

Scanning electron microscope (SEM) imagery of Brazos River lapilli and sublapilli reveals an interior with ~20% intergranular porosity between calcite crystals (Fig. 8). The crystals are mostly equidimensional in shape, ranging from rhombic to anhedral (Figs. 8C–8F). Small areas contain multicrystal units that appear as areas of uniform white color in BSE images. Pore spaces contain sparse smectite platelets in sponge-like arrays (Fig. 8E), resulting in a somewhat frothlike arrangement of platelets in pores. The outer rim of a lapillus (Figs. 8A and 8B) is more compact and has more cement, giving it greater mechanical strength than the interior regions.

The smectite platelets of interior pores are secondary, but solid masses of smectite (ranging in size from 10 to 500 μm), interpreted as areas of altered silicic glass (Figs. 5C and 5E), occur interspersed with the calcite crystal aggregates in carbonate accretionary lapilli. The smallest (10 μm) smectite masses (Figs. 5F and 5G) are round and have uniform composition, or they may contain other mineral components in the form of submicrometer-size particles. Larger smectite masses contain small calcite crystals scattered throughout. Masses of 100 μm or larger are heterogeneous in composition; most contain aggregates of calcite crystals of the same type as those present in the main body of the particle, indicating complex episodes of accretion during formation of carbonate accretionary lapilli.

DISTINGUISHING CARBONATE ACCRETIONARY LAPILLI FROM OTHER CARBONATE PARTICLES

The carbonate accretionary lapilli and sublapilli described here are mostly extracted from the Cretaceous-Paleogene boundary deposits at Brazos River, Texas, and much of the discussion about them comes from observations on occurrences at the Brazos River site, where the depositional environmental context of the deposits is well documented (Yancey, 1996; Schulte et al., 2006). Work on samples from Bass River borehole, New Jersey, and Mimbral, northern Mexico, provides additional data supporting the results from Brazos River samples. In unweathered samples, carbonate accretionary lapilli are white in reflected light, contrasting with the greenish or gray color of smectite-replaced altered glass spherules (Figs. 1C and 1D) and the dull white to gray color of carbonate-replaced spherules (Figs. 1B and 1D). The white coloration, due to the light-scattering properties of the component minute crystals, indicates that the crystals are smaller (Fig. 9A) than crystals of replacement carbonate present in the same deposits (Fig. 9C). Most of the carbonate accretionary sublapilli are fragments of larger lapilli and have one or more flat faces (Figs. 1A and 3C), producing a subangular, blocky form and indicating that breakage occurred before final deposition in the Cretaceous-Paleogene boundary deposits. The broken margins of sublapilli reveal the presence of darker spots with a dull luster (Fig. 1A) that are areas of higher smectite content. Once recognized, the white coloration in reflected light, subrounded form, and uniformity in appearance of the carbonate accretionary lapilli make them easy to distinguish and separate from other particles.

Ejecta particles in the Brazos River Cretaceous-Paleogene boundary deposits and other boundary deposits along the northwestern and northern parts of the Gulf of Mexico occur within redeposited sediments (Figs. 1E and 1F) that were transported in a slurry or grain suspension before they were deposited (Smit et al., 1996; Yancey, 1996). Therefore, carbonate accretionary lapilli can be mixed with carbonate particles of local detrital origin such as bioclasts, peloids, eroded bedrock lithoclasts, reworked concretions, or pedogenic carbonate nodules and must be distinguished from these locally derived particles. Bioclasts are easy to recognize because skeletal fragments retain distinctive skeletal morphology and shell microstructure (see Carter, 1990, for examples), and calcite bioclasts are well preserved in Cretaceous-Paleogene boundary deposits (Fig. 1E). Skeletal carbonate has crystals that are tightly intergrown (Carter, 1990), in contrast to the porous texture of carbonate accretionary lapilli (Fig. 8). Carbonate accretionary lapilli are distinguished from lithoclasts of eroded bedrock, peloids, or reworked concretion origin by their lack of fossil bioclast components, pore-filling spar, planar lamination, or recognizable detrital grains (features common to sedimentary carbonate; Scholle, 1978). The limited range of lapilli microfabric shown in Figures 4 and 5 has little overlap with microfabric of sedimentary carbonate, including the clotted microfabric observed in some limestones (Scholle, 1978).

The possibility that clasts of pedogenic carbonate could be present in the Brazos River and northern Mexico Cretaceous-Paleogene boundary deposits needs special attention and evaluation because some types of calcrete have a microfabric that is similar to that of carbonate accretionary lapilli. At the time of impact, the northern Mexico-Texas region was located in a semiarid climate zone where pedogenic carbonate would be expected. An accretionary microfabric could be confused with some pedogenic (calcrete/caliche) materials (Fig. 9B) because calcrete has such varied microfabric that any accretionary fabric can be matched with some example of calcrete (see Wright and Tucker, 1991), but the range of microfabric in the two types of materials is not the same. Although texture does not provide convincing evidence for or against an origin as calcrete clasts, the dissimilar ranges of microfabric provide strong circumstantial evidence against a subaerial pedogenic/calcrete origin for the white carbonate grains. The presence of these grains in Bass River, New Jersey, Cretaceous-Paleogene deposits, an area of humid climates, indicates that a pedogenic origin for carbonate accretionary lapilli is improbable.

The dominant size of calcite crystals in the carbonate accretionary lapilli is 1–4 μm, and this size fraction accounts for 80% or more of all calcite. The size of calcite crystals is not a direct indicator of origin, because single micrometer-sized calcite can form by precipitation or by recrystallization of preexisting carbonate. However, crystal size of recrystallized microspar is mostly in the 4–10 μm size range (Moshier, 1989), in contrast to the smaller size of calcite in carbonate accretionary lapilli. Calcite crystals of known replacement origin present in the Brazos River deposits are much larger (Figs. 9C and 10B), and biogenic calcite present in the same deposits is well preserved, with no indication of recrystallization. These factors do not rule out some recrystallization for the 1–4-μm-size calcite crystals, but they indicate the crystals are not replacements of other carbonate fabrics.

DISCUSSION

The formation of carbonate impact ejecta or carbonate melt during impact is known for a few sites, including the Chicxulub crater (Jones et al., 2000), Ries crater (Graup, 1999), Haughton

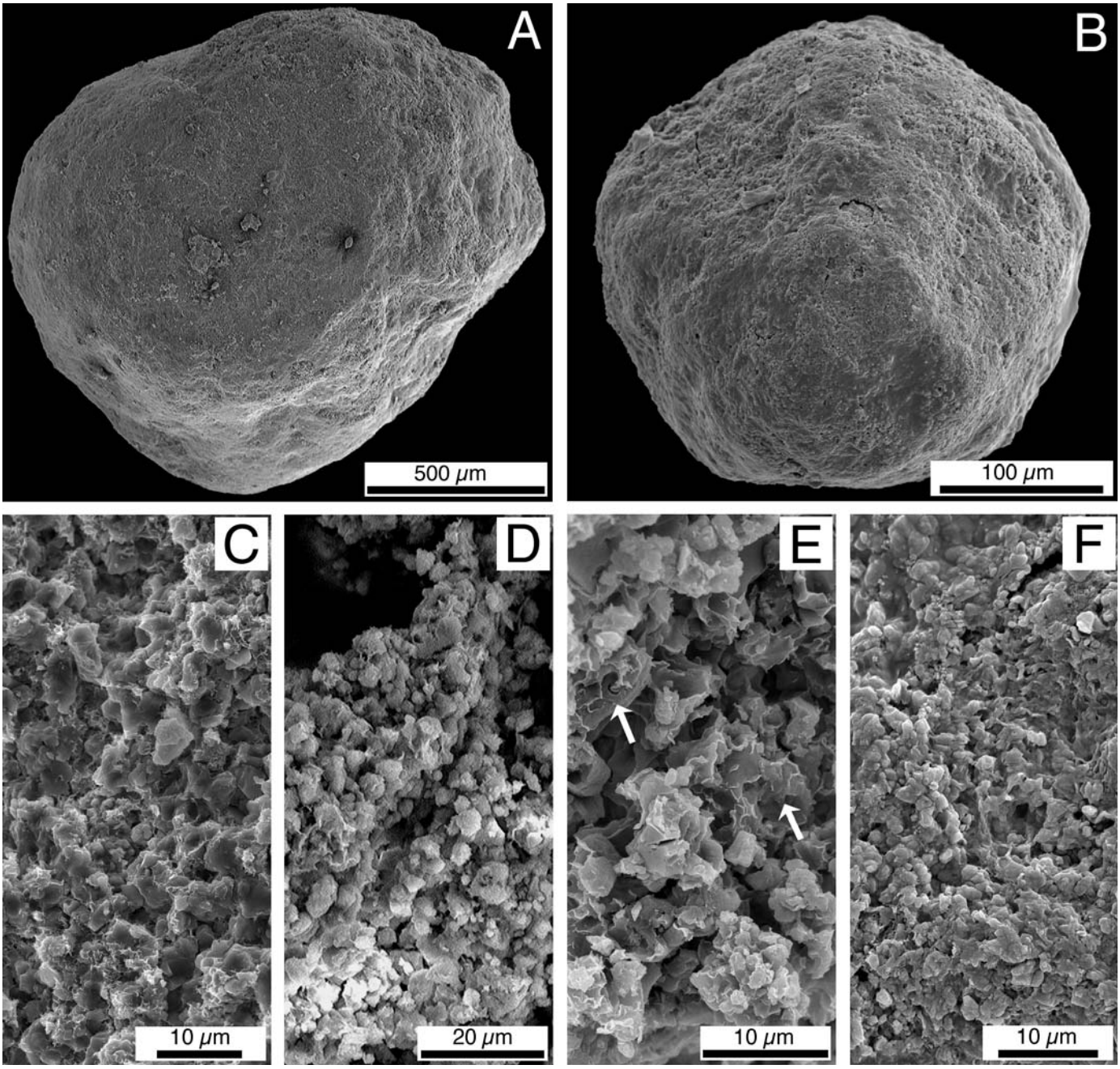

Figure 8. Scanning electron microscope (SEM) images of carbonate accretionary sublapilli, showing uniform appearance of exterior of sublapilli and small crystal size within interior, from Brazos River, Texas and Bass River borehole, New Jersey. (A) Whole carbonate accretionary sublapillus, showing uniform appearance of exterior, from spherule-rich layer in Brazos River section RB4B, Brazos River, Texas. (B) Whole carbonate accretionary sublapillus, showing uniform appearance of exterior of grain, from Bass River borehole, New Jersey. (C) Broken surface of interior of carbonate accretionary sublapillus, showing nearly uniform crystal size, from spherule-rich layer in Brazos River section RB4B, Brazos River, Texas. (D) Fragment of carbonate accretionary sublapillus, showing sparse smectite platelets in micropores in the interior of the particle, from spherule-rich layer, Darting Minnow Creek, Brazos River, Texas. (E) Fragment of carbonate accretionary sublapillus, showing grain microfabric and presence of sparse small smectite platelets (arrows) with edgewise attachment to calcite grains and each other in micropores in the interior of the particle, from spherule-rich layer, Darting Minnow Creek, Brazos River, Texas. (F) Detail of exterior surface of carbonate accretionary sublapillus shown in B, from Bass River borehole, New Jersey.

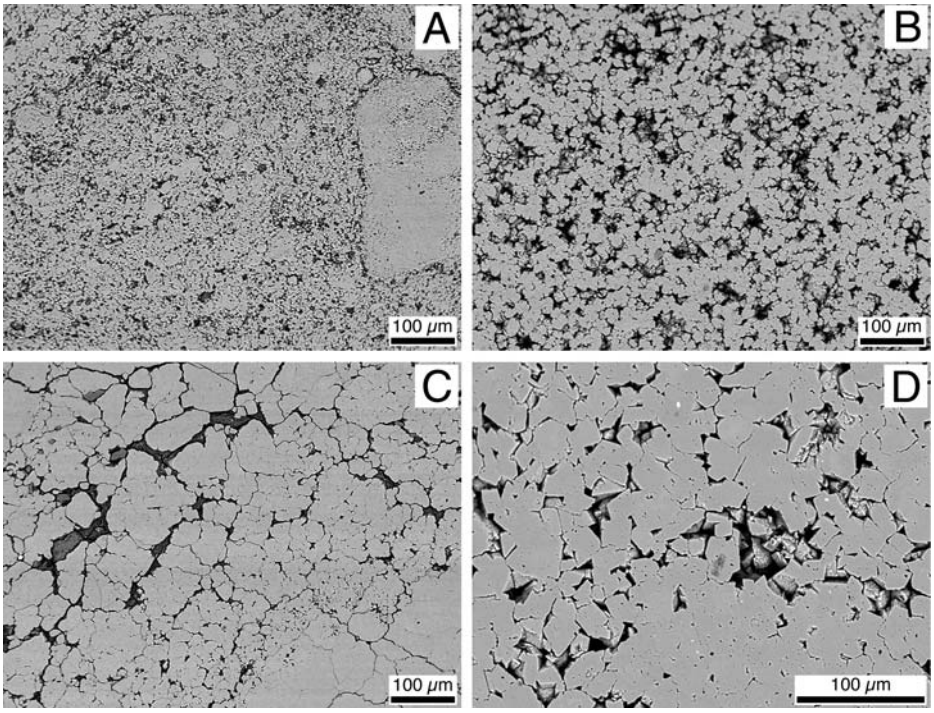

Figure 9. Backscattered electron (BSE) images comparing microfabrics of carbonate accretionary lapilli and secondary carbonate materials. (A) Microfabric of carbonate accretionary lapillus fragment from spherule-rich layer in Brazos River section RB4B, Brazos River, Texas. (B) Microgranular fabric of modern pedogenic calcrete soil nodule extracted from shale matrix, Park Road 15, Brown County, Texas. (C) Coarse irregular crystal fabric of calcite vein taken from carbonate-cemented portion of spherule-rich layer in Brazos River section RB4B, Brazos River, Texas. (D) Coarse fabric of dolomite-replaced spheroid from Albion Island Formation spheroid bed, Albion Island, Belize.

crater (Osinski and Spray, 2001), and the southern Nevada Alamo Breccia (Warme and Kuehner, 1998; Warme et al., 2002), but it is the Chicxulub and Late Devonian Alamo impacts into continental shelves covered with carbonate sediments that produced large amounts of carbonate accretionary lapilli. The Alamo impact event is of special interest because no silicic basement component occurs in the ejecta, and large quantities of carbonate accretionary lapilli were produced from impacted limestone bedrock. Warme and Kuehner (1998) and Warme et al. (2002) noted that the Alamo accretionary materials produced by the impact and distributed over a radius of 100 km from the probable impact site closely resemble volcanic accretionary lapilli. The Alamo impact occurred on a shallow shelf covered with ocean water and condensation of water onto the surface of ash particles is invoked to explain accretion of particles in impact-generated debris-laden clouds. This process could also apply to the Chicxulub impact, an event that occurred on a shallow ocean water–covered continental shelf (Goto et al., 2004, p. 1244). The Alamo accretionary lapilli range up to 3 cm in diameter, with a mean size of 0.5 cm, and they have an outer rim ("crust") composed of finer particles than the interior. The lapilli are concentrated in the upper parts of the Alamo Breccia deposits, indicating deposition late during the accumulation of slides, debris flows, and seismites produced as a consequence of the impact, as well as reworking of lapilli into younger beds.

Carbonate accretionary lapilli of the Chicxulub impact are comparable to those of the Alamo impact, and both resemble volcanic accretionary lapilli. Pope et al. (2005, p. 187) made a comparison of the Albion Island Formation spheroid bed deposits to volcanic pyroclastic deposits and noted the similarity of accretionary lapilli produced by impact to accretionary lapilli present in pyroclastic materials. Volcanic accretionary lapilli are produced in dense suspensions of particles within turbulent eruptive plumes and can form in diverse places within the plume. The formation of accretionary particles occurs where solid particles acquire a fluid coating that allows them to stick together (Gilbert and Lane, 1994; Schumacher and Schmincke, 1995) as they come into contact. Forces that promote accretion are liquid capillary forces on hygroscopic particles, derived from the presence of a thin water (or acid) coating, and electrostatic attraction of minute hot particles (Schumacher and Schmincke, 1995). Impact on a shallow-marine shelf site would generate substantial amounts of water vapor in the impact plume, enhancing the chance for accretion to occur.

Most of the Chicxulub carbonate accretionary lapilli contain altered masses of silicic glass, indicating co-occurrence of carbonate and silicic glass particles at the time of formation. Carbonate vapor/melt and silicate melt originate at different places within the crater, so intimate co-occurrence of these contrasting materials within the same particle indicates generation of accretionary particles in turbulent gases that mixed materials from various sites within the impact crater. Aggregation of Chicxulub impact-produced carbonate into accretionary lapilli differed from volcanic aggregation in one important way: the carbonate solids that aggregated to form small Chicxulub carbonate accretionary particles were composed primarily of calcite crystals in the 1–4 μm size range. The near uniformity and very small size of these calcite crystals suggest that the smallest particles involved in accretion were minute particles generated in impact vapors, not by accretion of irregularly shaped ash particles produced from melt or fragmentation.

Production of minute crystals of carbonate during impact into carbonate rocks is possible because of the types of chemical reactions that occur there. Agrinier et al. (2001) discussed the probable sequence of events, which begins with decomposition of carbonate and continues with chemical reactions and back-reactions that lead to regeneration of carbonate solids within the impact-generated vapor plume. Impact heating and volatilization are expected to release CO_2 from carbonate and to produce minute particles of powdered CaO as the carbonate mineral crystal structure is destroyed by volatilization. Decarbonized carbonate would not survive as recognizable bedrock clasts because of the powdering effect. At higher temperatures, hot powdered CaO can combine directly with CO_2, whereas at lower temperatures, it can react with H_2O to produce $Ca(OH)_2$ (Agrinier et al., 2001). In the CO_2-enriched vapor, $Ca(OH)_2$ can then react with CO_2 to produce $CaCO_3$ and water vapor, completing the back-reaction chain of events to generate $CaCO_3$. Reactions taking place in the vapor plume under these conditions are expected to produce minute crystals. Turbulent conditions in the plume provide the physical conditions needed to aggregate these solids into accretionary lapilli.

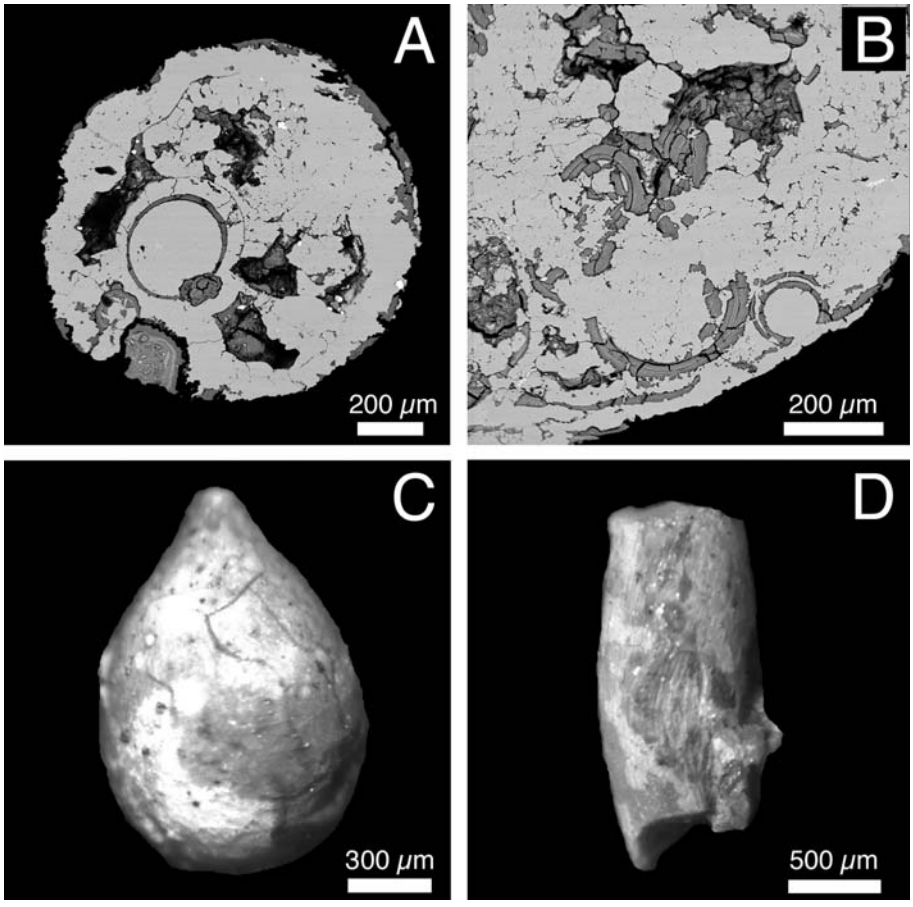

Figure 10. Backscattered electron (BSE) images of calcite-replaced bubble-bearing glass spherules (A, B) and reflected-light views of calcite-replaced glass droplets (C, D) from spherule-rich layer in Brazos River section RB4B, Brazos River, Texas. (A) Spherule with smectite-lined large bubble filled with calcite; remainder of spherule is coarse replacement calcite (light areas) and small irregular smectite-lined voids (dark areas); small bright white areas are pyrite. Original fabric has been mostly destroyed by alteration. (B) Portion of spherule with smectite lining on bubble walls that are fragmented by later calcite replacement of spherule. (C) Drop-shaped calcite-replaced glass spherule, with some shrinkage cracks showing on surface. (D) Portion of elongate calcite-replaced glass droplet with flow lines preserved on outer surface

Distribution of accretionary particles (carbonate or otherwise) is best known in the context of turbulent cloud transport, but, at best, this is a minor part of impact models. Numerical simulation of the Chicxulub impact, based on the amounts of energy available (Vickery and Melosh, 1990; Kring and Durda, 2002), indicates rapid movement of the vapor plume to a position outside the atmosphere and implies that within-atmosphere transport occurred primarily in the expanding debris-laden blast curtain moving along Earth's surface. Kring and Durda (2002) stated that ejecta carried more than 400 km from the site where it was launched was carried above the atmosphere in the vapor plume, and then the ejecta settled through the atmosphere to the surface. This implies that carbonate accretionary lapilli transported to distal sites (1000–2500 km) could have been formed only during the first few seconds of the impact blast. After the vapor plume expanded out of the impact crater and rose above the atmosphere, there would be little or no chance for particle accretion to occur. This situation is very limiting in reconstructing the events present during formation of carbonate accretionary lapilli transported beyond 400 km and difficult to reconcile with the inferred series of chemical reactions and physical accretion stages needed for their formation.

Comparisons with proximal Chicxulub accretionary lapilli show that the microfabric of carbonate accretionary lapilli and sublapilli of Brazos River and Bass River deposits is very similar to the microfabric of the smaller carbonate accretionary lapilli present in Albion Island Formation deposits (Fouke et al., 2002; Pope et al., 2005). The Albion Island Formation lapilli are interpreted to have formed within the surface-moving dense ejecta curtain, under conditions different from those in the vapor plume. Regardless of the differences in interpretation of environment of formation, it is reasonable to assume that similar-appearing carbonate accretionary lapilli deposited at 350 km (Belize), 1000 km (Brazos River), and 2500 km (Bass River) distances from Chicxulub were formed by similar processes. The available evidence indicates that the white carbonate particles of the Cretaceous-Paleogene boundary deposits are best interpreted as carbonate accretionary lapilli of primary microaccretionary origin, formed within the impact plume. They are small versions of the large carbonate accretionary lapilli and blocks present in the Chicxulub proximal ejecta deposits, as illustrated in Ocampo et al. (1996) and Pope et al. (2005).

We believe that there is reason to assign greater importance to a role for turbulent cloud transport in distributing Chicxulub impact ejecta. Bohor (1990) and Pollastro and Bohor (1993) suggested a significant role for turbulent cloud transport of Chicxulub ejecta, and Warme et al. (2002) invoked a within-atmosphere process for the formation of Alamo accretionary lapilli. An enhanced role for turbulent plume clouds in ejecta transport is supported by the co-occurrence of altered glass spherules (both with and without bubbles) and carbonate accretionary lapilli in the same deposits. The similar size and low density of altered bubble-bearing glass spherules (Figs. 1B, 10A, and 10B) are compatible with distribution by a turbulent plume cloud. Only the rare teardrop, dumbbell, or discoid shapes present at Brazos River (Figs. 10C and 10D), Haiti (Kring and Boynton, 1991), and Alabama (Pitakpaivan et al., 1994) suggest movement at high speed, but they have small mass and could easily have been caught up in turbulent plume clouds as well. Ejecta particles of all kinds at Brazos River and nearby sites and at more distant locations could have been transported by turbulent cloud suspension. The decrease in mean particle size with increasing distance from the crater (data for shocked quartz grains and bubble-containing glass spherules are summarized in Kring and Durda [2002]; carbonate accretionary lapilli data are presented here and in Pope et al. [2005]) suggests similarity of transport processes for carbonate accretionary lapilli, sublapilli, and bubble-bearing glass spherules.

CONCLUSIONS

Petrographic and electron-microprobe studies of carbonate ejecta in Cretaceous-Paleogene

boundary deposits at Brazos River, Texas, and Bass River, New Jersey, up to 2500 km from the Chicxulub impact site, show that many particles of carbonate composition in these deposits are carbonate accretionary lapilli and sublapilli. They are composed of micrometer-sized crystals of low-Mg calcite that accreted while in plume clouds generated by impact; they aggregated into clumps ranging from ten to several hundred micrometers in size, along with droplets of silicic glass (now altered to smectite), and so formed lapilli with accretionary clumps of varied sizes. Electron-microprobe analysis shows that lapilli have elevated S content, and the S is evenly distributed throughout the aggregates, probably contained in minute crystals adhering to calcite crystals. The analyzed concentration of Mg is high in small areas, and X-ray elemental distribution maps show that the Mg is present within submicrometer-sized grains. Analyses of these grains suggest that the Mg is possibly present as MgO (periclase) and not Mg-carbonate, and we believe that MgO could have formed in the vapor cloud along with calcite. Further work is needed to confirm the exact identity of this high-Mg phase. The calcite crystals are half the size of diagenetic calcite microspar crystals and are of the size expected to form in a vapor plume. This is taken as evidence that they formed as original calcite in the impact plume and are not diagenetic in origin.

Carbonate accretionary lapilli co-occur with bubble-bearing altered glass spherules in the area of study from Mimbral, Mexico, to Bass River borehole, New Jersey, and in other sites along the Gulf of Mexico coastal plains, indicating a similar time of formation and deposition. The data presented here lead to the conclusion that a large amount of carbonate particulate material was generated by the Chicxulub impact event and that accretionary lapilli, composed of carbonate and smaller amounts of silicic glass particles, formed in abundance during dispersal from the crater. The co-occurrence and similar mean sizes of ejecta particles at sites distant from the impact suggest that large turbulent, ejecta-laden plume clouds could have had a substantial role in transporting small Chicxulub ejecta of all types for thousands of kilometers from the impact site.

ACKNOWLEDGMENTS

We are most grateful to Richard Olsson, Rutgers University, for providing two samples of the Cretaceous-Paleogene boundary spherule layer in the Bass River borehole that gave us confirmation that carbonate accretionary lapilli are widespread in Cretaceous-Paleogene boundary deposits. David King, Auburn University, provided samples of spheroids from the Albion Island quarry, Belize, for comparison with Brazos River samples. Gerta Keller, Princeton University, provided small samples of spherule material from the Brazos River Mullinax #1 core drilled in March 2005 (National Science Foundation [NSF] grant 0447171) and the outcrop at Mimbral and gave permission to use photographs of the core. Brian Huber, National Museum of Natural History, loaned small samples of Cretaceous-Paleogene boundary deposits from Blake Nose Ocean Drilling Program (ODP) site 1049, but carbonate particles suspected to be carbonate accretionary lapilli were too small and too altered to provide data for this project. We are indebted to John Warme, Bruce Simonson, and Alex Wittmann for helpful comments that contributed greatly to improving this paper. This study was supported in part by the Electron Microprobe Laboratory of the Department of Geology and Geophysics, Texas A&M University.

REFERENCES CITED

Agrinier, P., Deutsch, A., Schaerer, U., and Martinez, I., 2001, Fast back-reactions of shock-released CO_2 from carbonates: An experimental approach: Geochimica et Cosmochimica Acta, v. 65, p. 2615–2632, doi: 10.1016/S0016-7037(01)00617-2.

Alvarez, W., Claeys, P., and Kieffer, S.W., 1995, Emplacement of Cretaceous-Tertiary boundary shocked quartz from Chicxulub crater: Science, v. 269, p. 930–935, doi: 10.1126/science.269.5226.930.

Bohor, B.F., 1990, Shock-induced microdeformations in quartz and other mineralogical indications of an impact event at the Cretaceous-Tertiary boundary: Tectonophysics, v. 171, p. 359–372, doi: 10.1016/0040-1951(90)90110-T.

Carter, J.G., 1990, Skeletal biomineralization: Patterns, processes and evolutionary trends: Volume 1: New York, Van Nostrand Reinhold Co., 832 p.

Claeys, P., Kiessling, W., and Alvarez, W., 2002, Distribution of Chicxulub ejecta at the Cretaceous-Tertiary boundary, *in* Koeberl, C., and MacLeod, K.G., eds., Catastrophic events and mass extinctions: Impacts and beyond: Geological Society of America Special Paper 356, p. 55–68.

Fouke, B.W., Zerkle, A.L., Alvarez, W., Pope, K.O., Ocampo, A.C., Wachtman, R.J., Grajales-Nishimura, J.M., Claeys, P., and Fischer, A.G., 2002, Cathodoluminescence petrography and isotope geochemistry of KT impact ejecta deposited 360 km from the Chicxulub crater, at Albion Island, Belize: Sedimentology, v. 49, p. 117–138, doi: 10.1046/j.1365-3091.2002.00435.x.

Gilbert, J.S., and Lane, S.J., 1994, The origin of accretionary lapilli: Bulletin of Volcanology, v. 56, p. 398–411.

Goto, K., Tada, R., Tajika, E., Bralower, T.J., Hasegawa, T., and Matsui, T., 2004, Evidence for ocean water invasion into the Chicxulub crater at the Cretaceous/Tertiary boundary: Meteoritics & Planetary Science, v. 39, p. 1233–1247.

Graup, G., 1999, Carbonate-silicate liquid immiscibility upon impact melting: Ries Crater, Germany: Meteoritics & Planetary Science, v. 34, p. 425–438.

Guillemette, R.N., and Yancey, T.E., 2006, Microaccretionary and accretionary carbonate spherules of the Chicxulub impact event from Brazos River, Texas, and Bass River, New Jersey: Houston, Lunar and Planetary Institute, Lunar and Planetary Science Conference XXXVII, abstract 1779 (CD-ROM).

Guillemette, R.N., and Yancey, T.E., 2007, Primary and diagenetic characteristics of Chicxulub impact ejecta spherules in the northwestern Gulf of Mexico: Houston, Lunar and Planetary Institute, Lunar and Planetary Science Conference XXXVIII, abstract 2218 (CD-ROM).

Jarosewich, E., 2002, Smithsonian microbeam standards: Journal of Research of the National Institute of Standards and Technology, v. 107, p. 681–685.

Jones, A.P., Claeys, P., and Heuschkel, S., 2000, Impact melting of carbonates from the Chicxulub crater, *in* Gilmour, I., and Koeberl, C., eds., Impacts and the early Earth: New York, Springer, p. 343–361.

Koeberl, C., 1993, Chicxulub crater, Yucatan: Tektites, impact glasses, and the geochemistry of target rocks and breccias: Geology, v. 21, p. 211–214, doi: 10.1130/0091-7613(1993)021<0211:CCYTIG>2.3.CO;2.

Kring, D.A., and Boynton, W.V., 1991, Altered spherules of impact melt and associated relic glass from K/T boundary sediments in Haiti: Geochimica et Cosmochimica Acta, v. 55, p. 1737–1742, doi: 10.1016/0016-7037(91)90143-S.

Kring, D.A., and Durda, D.D., 2002, Trajectories and distribution of materials ejected from the Chicxulub impact crater: Implications for post-impact wildfires: Journal of Geophysical Research, v. 107, no. E8, p. 6.1–6.22.

Kyte, F.T., Bostwick, J.A., and Zhou, L., 1996, The Cretaceous-Tertiary boundary on the Pacific plate: Composition and distribution of impact debris, *in* Ryder, G., et al., eds., The Cretaceous-Tertiary event and other catastrophes in Earth history: Geological Society of America Special Paper 307, p. 389–401.

Morrow, J.R., Sandberg, C.A., and Harris, A.G., 2005, Late Devonian Alamo impact, southern Nevada, USA: Evidence of size, marine site, and widespread effects, *in* Kenkmann, T., et al., eds., Large meteorite impacts III: Geological Society of America Special Paper 384, p. 259–280.

Moshier, S.O., 1989, Microporosity in micritic limestones: A review: Sedimentary Geology, v. 63, p. 191–213, doi: 10.1016/0037-0738(89)90132-2.

Ocampo, A.C., Pope, K.O., and Fischer, A.G., 1996, Ejecta blanket deposits of the Chicxulub crater from Albion Island, Belize, *in* Ryder, G., et al., eds., The Cretaceous-Tertiary event and other catastrophes in Earth history: Geological Society of America Special Paper 307, p. 75–88.

Olsson, R.K., Miller, K.G., Browning, J.V., Habib, D., and Sugarman, P.J., 1997, Ejecta layer at the Cretaceous-Tertiary boundary, Bass River, New Jersey (Ocean Drilling Program Leg 174AX): Geology, v. 25, p. 759–762, doi: 10.1130/0091-7613(1997)025<0759:ELATCT>2.3.CO;2.

Olsson, R.K., Miller, K.G., Browning, J.V., Wright, J.D., and Cramer, B.S., 2002, Sequence stratigraphy and sea-level change across the Cretaceous-Tertiary boundary on the New Jersey passive margin, *in* Koeberl, C., and MacLeod, K.G., eds., Catastrophic events and mass extinctions: Impacts and beyond: Geological Society of America Special Paper 356, p. 97–108.

Osinski, G.R., and Spray, J.G., 2001, Impact-generated carbonate melts: Evidence from the Haughton structure, Canada: Earth and Planetary Science Letters, v. 194, p. 17–29, doi: 10.1016/S0012-821X(01)00558-1.

Pitakpaivan, K., Byerly, G.R., and Hazel, J.E., 1994, Pseudomorphs of impact spherules from a Cretaceous-Tertiary boundary section at Shell Creek, Alabama: Earth and Planetary Science Letters, v. 124, p. 49–56, doi: 10.1016/0012-821X(94)00077-8.

Pollastro, R.M., and Bohor, B.F., 1993, Origin and clay mineral diagenesis of the Cretaceous/Tertiary boundary unit, western interior of North America: Clays and Clay Minerals, v. 41, p. 7–25, doi: 10.1346/CCMN.1993.0410102.

Pope, K.O., Ocampo, A.C., Fischer, A.G., Alvarez, W., Fouke, B.W., Webster, C.L., Vega, F.J., Smit, J., Fritsche, A.E., and Claeys, P., 1999, Chicxulub impact ejecta from Albion Island, Belize: Earth and Planetary Science Letters, v. 170, p. 351–364, doi: 10.1016/S0012-821X(99)00123-5.

Pope, K.O., Ocampo, A.C., Fischer, A.G., Vega, F.J., Ames, D.E., King, D.T., Jr., Fouke, B.W., Wachtman, R.J., and Kletetschka, G., 2005, Chicxulub impact ejecta deposits in southern Quintana Roo, Mexico, and central Belize, *in* Kenkmann, T., et al., eds., Large meteorite impacts III: Geological Society of America Special Paper 384, p. 171–190.

Rocchia, R., Robin, E., Froget, L., and Gayraud, J., 1996, Stratigraphic distribution of extraterrestrial markers at the Cretaceous-Tertiary boundary in the Gulf of Mexico area: Implications for the temporal complexity of the event, *in* Ryder, G., et al., eds., The Cretaceous-Tertiary event and other catastrophes in Earth history: Geological Society of America Special Paper 307, p. 279–286.

Salge, T., 2007a, The ejecta blanket of the Chicxulub impact crater, Yucatán, Mexico: Petrographic and chemical studies of the K-P section of El Guayal and UNAM boreholes [Ph.D. Thesis]: Berlin, Humboldt-Universität zu Berlin, Mathematisch-Naturwissenschaftliche Fakultät I, 130 p., http://edoc.hu-berlin.de/docviews/abstract.php?id=27753.

Salge, T., 2007b, The ejecta blanket of the Chicxulub impact crater: Petrographic and chemical studies of the K-P section of El Guayal and of the UNAM boreholes: Houston, Lunar and Planetary Institute, Lunar and Planetary Science Conference XXXVIII, abstract 1748 (CD-ROM).

Scholle, P.A., 1978, A color illustrated guide to carbonate rock constituents, textures, cements, and porosities: American Association of Petroleum Geologists Memoir 27, 241 p.

Schulte, P., Speijer, R., Mai, H., and Kontny, A., 2006, The Cretaceous-Paleogene (K-P) boundary at Brazos, Texas: Sequence stratigraphy, depositional events and the Chicxulub impact: Sedimentary Geology, v. 184, p. 77–109, doi: 10.1016/j.sedgeo.2005.09.021.

Schumacher, R., and Schmincke, H.U., 1995, Models for the origin of accretionary lapilli: Bulletin of Volcanology, v. 56, p. 626–639.

Smit, J., Roep, T.B., Alvarez, W., Montanari, A., Claeys, P., Grajales-Nishimura, J.M., and Bermudez, J., 1996, Coarse-grained, clastic sandstone complex at the KT boundary around the Gulf of Mexico: Deposition by tsunami waves induced by the Chicxulub impact?, *in* Ryder, G., et al., eds., The Cretaceous-Tertiary event and other catastrophes in Earth history: Geological Society of America Special Paper 307, p. 151–182.

Vickery, A.M., and Melosh, H.J., 1990, Atmospheric erosion and impactor retention in large impacts, with application to mass extinctions, *in* Sharpton, V.L., and Ward, P.D., eds., Global catastrophes in earth history—An interdisciplinary conference on impacts, volcanism, and mass mortality: Geological Society of America Special Paper 247, p. 289–300.

Warme, J.E., and Kuehner, H.-C., 1998, Anatomy of an anomaly: The Devonian catastrophic Alamo impact breccia of southern Nevada: International Geology Review, v. 40, p. 189–216.

Warme, J.E., Morgan, M., and Kuehner, H.-C., 2002, Impact-generated carbonate accretionary lapilli in the Late Devonian Alamo Breccia, *in* Koeberl, C., and MacLeod, K.G., eds., Catastrophic events and mass extinctions: Impacts and beyond: Geological Society of America Special Paper 356, p. 489–504.

Wright, V.P., and Tucker, M.E., 1991, Calcretes: Boston, Blackwell Scientific Publishers, 352 p.

Yancey, T.E., 1996, Stratigraphy and depositional environments of the Cretaceous-Tertiary boundary complex and basal Paleocene section, Brazos River, Texas: Transactions of the Gulf Coast Association of Geological Societies, v. 46, p. 433–442.

Yancey, T.E., 2002, Carbonate ejecta spherules in Cretaceous-Tertiary boundary deposits, Brazos River, Texas: Geological Society of America Abstracts with Programs, v. 34, no. 6, p. 402.

Manuscript Received 9 November 2006
Revised Manuscript Received 7 March 2008
Manuscript Accepted 28 March 2008

Printed in the USA